Microwave-Frequency Experiment Validation of a Novel Magneto-Photonic Crystals Circulator

Wang, Yong; Zhang, Dengguo; Xu, Shixiang; Xu, Biaogang; Dong, Zheng; Xue, Quan

Published in:
IEEE Photonics Journal

Published: 01/06/2018

Document Version:
Final Published version, also known as Publisher's PDF, Publisher's Final version or Version of Record

Published version (DOI):
10.1109/JPHOT.2017.2783341

Publication details:
Wang, Y., Zhang, D., Xu, S., Xu, B., Dong, Z., & Xue, Q. (2018). Microwave-Frequency Experiment Validation of a Novel Magneto-Photonic Crystals Circulator. *IEEE Photonics Journal*, *10*(3), [5300106]. https://doi.org/10.1109/JPHOT.2017.2783341

IEEE Photonics Journal
An IEEE Photonics Society Publication

Open Access

Microwave-Frequency Experiment Validation of a Novel Magneto-Photonic Crystals Circulator

Volume 10, Number 3, June 2018

Yong Wang
Dengguo Zhang
Shixiang Xu
Biaogang Xu
Zheng Dong
Quan Xue, *Fellow, IEEE*

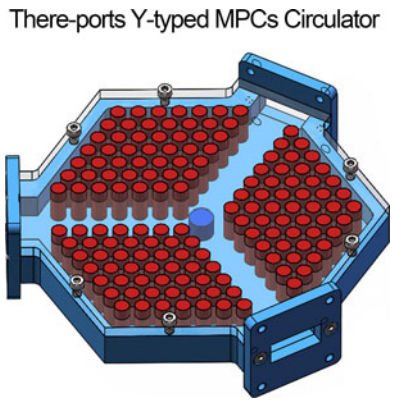

DOI: 10.1109/JPHOT.2017.2783341
1943-0655 © 2017 IEEE

IEEE photonics SOCIETY

IEEE

Microwave-Frequency Experiment Validation of a Novel Magneto-Photonic Crystals Circulator

Yong Wang,[1] Dengguo Zhang,[2] Shixiang Xu,[2] Biaogang Xu,[2] Zheng Dong,[2] and Quan Xue,[3] *Fellow, IEEE*

[1]College of Optoelectronic Engineering, Shenzhen University, Shenzhen 518060, China
[2]College of Electronic Science and Technology, Shenzhen University, Shenzhen 518060, China
[3]Department of Electronic Engineering, City University of Hong Kong, Hong Kong

DOI:10.1109/JPHOT.2017.2783341

Manuscript received September 15, 2017; revised November 21, 2017; accepted December 11, 2017. Date of publication December 14, 2017; date of current version June 4, 2018. This work was supported by the National Natural Science Foundation of China under Grant 61171006. Corresponding author: D. G. Zhang (e-mail: dgzhang@szu.edu.cn).

Abstract: A novel three-port Y-shaped circulator based on magneto-photonic crystals is first experimentally investigated. The band gaps of TE mode for the photonic crystals are calculated by plane wave expansion method. The transmission characteristics of the circulator are simulated by finite element method and the experiments are performed in the microwave regime. At the central frequency of 9.83 GHz, the optimal experimental isolation of –61.11 dB is better than the numerical results.

Index Terms: Photonic crystal, circulator, magneto-photonic system, nonreciprocal device.

1. Introduction

Circulators are nonreciprocal devices used in communication systems, which can suppress multiple reflections between components and thereby improve tolerance with respect to fabrication imperfections and environmental fluctuations [1]–[7]. In the past few years, circulators based on photonic crystals (PCs) [8], [9], have been vigorously studied due to their excellent performances and promising applications. In 2005, a three-port photonic crystal circulator was first proposed by coupling a single magneto-photonic crystals (MPCs) cavity and introducing air holes array in bismuth iron garnet (BIG) [10]. Then, a type of carefully designed MPCs cavity was used to realize Y-format and W-format circulators [11], [12]. The T-typed and cross-typed circulators have also been designed [13]. The circulators with three and four ports for sub-terahertz region are designed by using silicon-ferrite MPCs [14]. Isolation, insertion loss and bandwidth are the most important performance parameters for circulators. A magnetically tunable circulator with high isolation of 65.2 dB is obtained by using two dimensional (2D) rods array [15]. In order to realize a Y-typed PCs circulator with ultra-low loss, a more compact structure with only one ferrite post in the central position of the waveguide junction was provided by us [16]. From above, it is evident that MPCs can provide great flexibilities in the design of circulators. Unfortunately, the study of PCs circulator until now is still at the stage of numerical simulation.

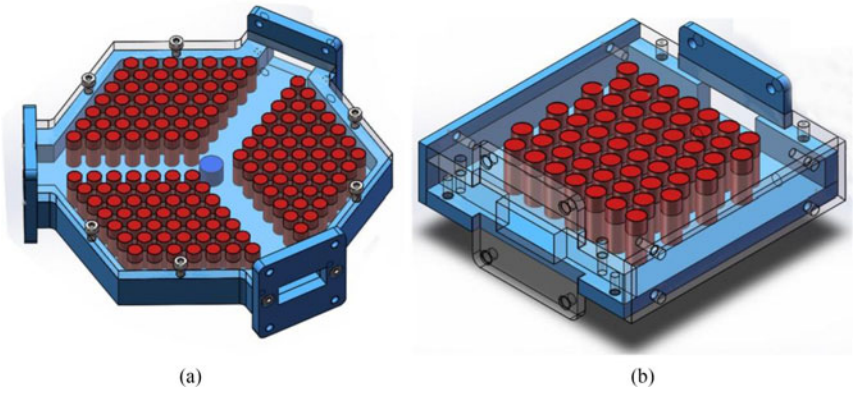

Fig. 1. (a) Structural diagram of the MPCs circulator in partially transparent waveguide; (b) Structural diagram of 7 × 8 TLPCs.

A 30 mm Y-junction MPCs circulator with low insertion loss of 0.062 dB is designed by using triangular lattice rods array [16]. Based on the dielectric rods model in [16], a new three-port Y-typed circulator based on Al_2O_3-ferrite MPCs is envisaged in this work. Due to the convenience and feasibility of the microwave-frequency experiment, the authors perform experiments to validate the PBG of the PCs and the function of the circulator in the microwave regime. The band gaps of TE modes for the triangular lattice Al_2O_3 PCs are calculated by plane wave expansion method. The characteristics of the circulator are simulated at the operating frequency of 9.8 GHz which is within the first photonic band gap (PBG). The numerical results show that the isolation and insertion loss of the circulator are −28.56 dB and −0.02 dB respectively. At the frequency of 9.83 GHz, the optimal experimental isolation value is up to −61.11 dB.

In order to validate the numerical results of the designed MPCs circulator, the microwave-frequency experiments are performed by using an Agilent E8361C vector network analyzer. At the frequency of 9.83 GHz, the optimal experimental isolation is up to −61.11 dB; the insertion loss of the circulator is −4.09 dB; the bandwidth is 105 MHz. The new Y-shaped MPCs circulator is envisaged and is first experimentally developed in the microwave regime in this short paper.

2. Numerical Calculation Results

The MPCs circulator is composed by putting nonreciprocal sample at the central point of the waveguide Y-shaped junction, as shown in Fig. 1(a). The structural diagram of 7 × 8 triangular lattice photonic crystals (TLPCs) is shown in Fig. 1(b). The MPCs are formed by introducing a Ni-Zn ferrite cylinder (blue) in the central of the TLPCs with Al_2O_3 rods (red). Under the external DC magnetic field, not only does the ferrite cylinder plays the role of a resonator, but also provides a 120° Faraday rotation angle. The lattice constant of the PCs is $a = 8$ mm. The Al_2O_3 rods' radius is $r_0 = 3$ mm with relative permittivity $\varepsilon_a = 9$. In the partially transparent hexagonal waveguide, the rods of MPCs are fixed on the upper and bottom plates. At the end of the waveguide, three Flange interfaces (22.86 × 10.16 mm) are designed to connect the test equipment.

To confirm the photonic band gap (PBG) of the TLPCs, a structure is discussed firstly. As shown in Fig. 1(b), the basic ingredient of the TLPCs is a 7 × 8 triangular lattice rods array distributed in the air. The lattice constant of the TLPCs and rod's radius are the same with those of the circulator mentioned above.

By using commercially available photonic band calculation software (BandSOLVE, Rsoft Design Group), the band structure of the 2D TLPCs is simulated with plane wave expansion method. The numerical analysis is carried out here only for TE polarization. The TE band structures of the Al_2O_3 TLPCs are shown in Fig. 2. As shown in Fig. 2, there are three PBGs in the TLPCs within the normalized frequency range of $0 \sim 0.8(2\pi c/a)$. In this work, the authors pay attention to validating the first PBG of $0.2380 \sim 0.2823(2\pi c/a)$. The central frequency of the first PBG is 9.76 GHz calcu-

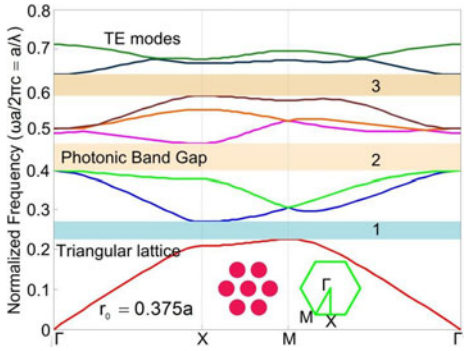

Fig. 2. The TE band structures of the Al_2O_3 TLPCs.

lated by 0.26(2πc/a) with the light speed c $= 3 \times 10^8$ m/s. In principle, PCs forbid the propagation of the electromagnetic waves within these PBG frequency ranges and reflect impinging electromagnetic waves back. The authors have performed experiment to validate the PBG of the TLPCs, as shown in Fig. 4(a). The experimental results show that there is a PBG of 9.77 ∼ 9.91 GHz. At the central frequency of 9.8 GHz, the isolation of the TLPCs reaches −37.53 dB and about 80% energy is reflected back to the input port. If a line defect waveguide junction is formed and at the central point some nonreciprocal sample such as ferrite post biased external magnet is situated, a circulator with 2D MPCs structure can be realized in the frequency of the PBG.

For a gyrotropic ferrite sample magnetized in the z-direction in microwave [17], the permeability tensor $[\mu_r]$ in the Cartesian co-ordinate system is:

$$[\mu_r] = \mu_0 \begin{bmatrix} \mu & j\kappa & 0 \\ -j\kappa & \mu & 0 \\ 0 & 0 & 1 \end{bmatrix} \tag{1}$$

Elements in the above tensor are

$$\mu = 1 + \frac{\omega_0 \omega_m}{\omega_0^2 - \omega^2} \tag{2}$$

$$\kappa = \frac{\omega \omega_m}{\omega_0^2 - \omega^2} \tag{3}$$

where $\omega_0 = \mu_0 \gamma H_0$ is the precession frequency and $\omega_m = \mu_0 \gamma M_s$. While H_0 is the bias magnetic field; $\gamma = 1.759 \times 10^{11}$ C/kg is the gyro-magnetic ratio; $M_s = 2.39 \times 10^5$ A/m is the saturation magnetization.

Traditionally, the frequency range of a circulator and its central frequency are determined by solving the tensor Maxwell's equation in ferrite under a given magnetic bias with the given boundary conditions. Owing to the complexity of the permeability tensor given in (1), the equations involved are extremely complex. It is doubtful whether the equations can be solved in a closed form. For a waveguide Y-junction circulator with a ferrite cylinder, Owen [18] showed that the central frequency of the circulator is approximately equal to the resonant frequency of the ferrite cylinder as if the latter was treated as a dielectric resonator. Following this theory, the ferrite cylinder in Fig. 1(a) is first examined as a dielectric resonator and designed in PCs waveguide's junction. A simple formula is derived to determine the central frequency of a magnetized ferrite cylinder [19], in which the relationship between the radius and height of the ferrite cylinder is given:

$$R = x \Big/ \left\{ \left(2\pi\sqrt{\varepsilon_f}/299.793\right)^2 - \left[\left(\pi/l_f\right) \times 1.5\right]^2 \right\}^{1/2} \tag{4}$$

where $\varepsilon_f = 13.6$ is relatively permittivity of the Ni-Zn ferrite; l_f is the height of the central ferrite with radius R; x is a compromise value [19], to ensure a suitable size of the ferrite cylinder for the

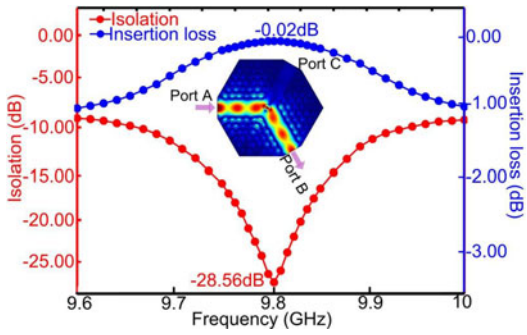

Fig. 3. Numerical isolation and insertion loss of the circulator.

junction of circulator, the x is chosen to be 2.4 here. In that way, the ferrite cylinder is designed firstly based on the given central frequency. Since the isolation of the TLPCs reaches -37.53 dB at the frequency of 9.8 GHz, as mentioned above, the central frequency of the circulator is also chosen to be 9.8 GHz. The height of the central ferrite cylinder is calculated to be 8.13 mm with the radius $R = 4.7$ mm.

Before experimentally validating the MPCs circulator, the external properties of the circulator are simulated at the frequency of 9.8 GHz by finite element method (Comsol Multiphysics). The external DC magnetic field $H_0 = 2.55 \times 10^5$ A/m is biased along z-direction on the ferrite post. The calculated region is divided into about 112 thousand grid cells and is encircled by perfect matched layers (PML) with double lattice constants thickness. Numerical isolation and insertion loss of the circulator is shown in Fig. 3. In the center of Fig. 3, Port A, B and C represent the three ports of the circulator. Under the external magnetic field bias, the propagation direction of the electromagnetic wave has a 120 degree deflection to realize 120 degree circulation. Therefore, the electromagnetic wave launched from Port A is almost totally transmitted to Port B (the output port); Port C is isolated.

The external characteristic parameters of the circulator are investigated by changing the frequency of incident electromagnetic wave. When signal is launched from one of the three ports (Port A, B and C), we gather the energy of signal at the other two ports and calculated the isolation and insertion loss of the circulator. The variations of the insertion loss and isolation with frequency for the MPCs circulator are already shown in Fig. 3. At the central frequency of 9.8 GHz, the isolation reaches -28.56 dB and the insertion loss is only -0.02 dB. When frequency diverges from the central frequency, the transmission characteristics of the circulator deteriorate gradually with increasing frequency offset.

3. Experimental Values

The validated experiments for MPCs circulator are divided into two steps. Firstly, the PBG of the TLPCs will be experimentally confirmed, as shown in Fig. 4(a). The detailed test method had been described similarly in [20], which is no longer repeated here. As shown in Fig. 4(b) is the top view of the MPCs circulator sample. Secondly, experimental setups for measuring the transmission characteristics of the MPCs circulator are shown in Fig. 4(c) and (d). The circulator and the vector network analyzer are connected through SMA connector and waveguide to coaxial converter. Under the action of permanent magnet (NdFeB), the transmission characteristics of the MPCs circulator are measured at the frequency range of 9.6 to 10 GHz, as shown in Fig. 5.

In the experiments, the parameter S_{21} represents logarithmic value of the ratio of the transmission power of Port 2 from the input power of Port 1. Similarly, S_{12} represents the transmission characteristic of the Port 2 to Port 1. In the classical measurement of the network analyser, the S parameters are respectively expressed as followings:

$$S_{21} = 10\lg\left(P_{21}/P_1\right) \tag{5}$$

$$S_{12} = 10\lg\left(P_{12}/P_2\right) \tag{6}$$

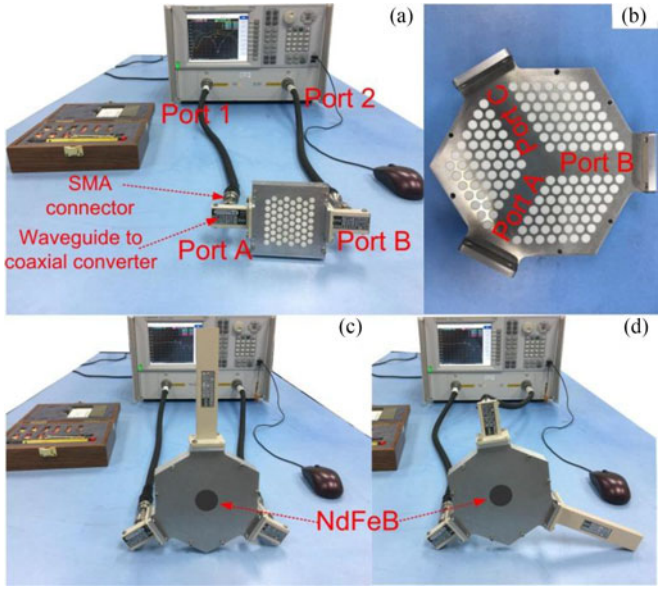

Fig. 4. (a) Experiment setup for measuring the PBG of the TLPCs; (b) top view of the MPCs circulator; (c) experimental setup for measuring transmission characteristics of Port A and Port B of the MPCs circulator; (d) experimental setup for measuring transmission characteristics of Port A and Port C of the MPCs circulator.

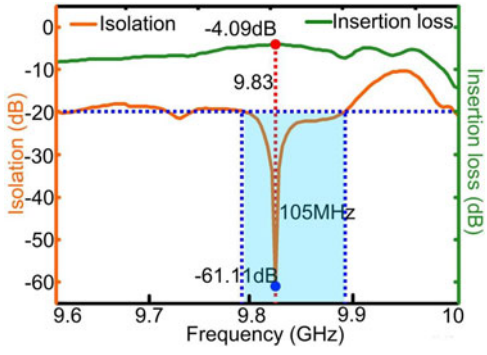

Fig. 5. Measured isolation and insertion loss of the circulator.

where P_1 and P_2 are the input power of the Port 1 and Port 2. P_{21} is the transmission power from Port 1 to Port 2 and P_{12} is the transmission power from Port 2 to Port 1.

In Fig. 4(c), Port 1 and Port 2 of the vector network analyzer are connected to Port A and Port B of the circulator. When the insertion loss of the electric cable and adapter is ignored, the isolation α_{BA} and insertion loss τ_{BA} of the circulator are respectively expressed as:

$$\tau_{BA} = S_{21} = 10\lg(P_{21}/P_1) \tag{7}$$

$$\alpha_{BA} = S_{12} = 10\lg(P_{12}/P_2) \tag{8}$$

When electromagnetic waves launched from Port A are transmitted to Port B (the output port), Port C is isolated. The measured isolation and insertion loss of the circulator are shown in Fig. 5. At the central frequency of 9.83 GHz, the measured insertion loss τ_{BA} is -4.09 dB; the isolation of the Port C to Port A is -61.11 dB. As shown in Fig. 5, the bandwidth of the circulator is about 105 MHz ($\alpha < -20$ dB). The experimental results perfectly agree with the numerical results mentioned above. In addition, the optimal experimental isolation of -61.11 dB is better than the numerical value.

4. Conclusion

In this short paper, a Y-shaped 2D MPCs circulator is designed and measured by using a Ni-Zn ferrite post and TLPCs. The TLPCs formed by Al_2O_3 ceramic rods array has a PBG of 9.77 $\sim$ 9.91 GHz. The central frequency of the circulator is determined by the height and radius of central ferrite resonator. The MPC circulator is first developed at the frequency range of 9.83 GHz. The excellent performance of the circulator demonstrates that 2D MPCs is a feasible method for developing nonreciprocal devices in microwave and millimeter wave band.

Photonic crystals show notable features in its ability to control motion of photonic, is considered the core of the future development of integrated photonics and optical communications. MPCs circulator, as one kind of non-reciprocal passive device, can be used to isolate the reflected light between adjacent devices or modules, in order to reduce interference and enhance the stability of large scale integrated optical circuit. Due to its special property, circulator is also widely used in high-resolution radar, radio astronomy and high speed data communications systems.

References

[1] E. J. Denlinger, "Design of partial height ferrite waveguide circulators," *IEEE Trans. Microw. Theory Techn.*, vol. 22, no. 8, pp. 810–813, Aug. 1974.

[2] Y. Akaiwa, "Operation modes of a waveguide Y circulator," *IEEE Trans. Microw. Theory Techn.*, vol. 22, no. 11, pp. 954–960, Nov. 1974.

[3] P. Pintus, F. D. Pasquale, and J. E. Bowers, "Integrated TE and TM optical circulators on ultra-low-loss silicon nitride platform," *Opt. Express*, vol. 21, no. 4, pp. 5041–5052, Feb. 2013.

[4] T. R. S. Santini, T. S. Ibrahim, and C. D. Maciel, "Load-insensitive active quasi-circulator for continuous-wave Doppler ultrasound applications," *Electron. Lett.*, vol. 52, no. 22, pp. 1823–1824, Oct. 2016.

[5] S. W. Y. Mung and W. S. Chan, "Active three-way circulator using transistor feedback network," *IEEE Microw. Wireless Compon. Lett.*, vol. 27, no. 5, pp. 476–478, Apr. 2017.

[6] T. S. Qiu, J. F. Wang, Y. F. Li, and S. B. Qu, "Circulator based on spoof surface plasmon polaritons," *IEEE Antennas Wireless Propag. Lett.*, vol. 16, no. 10, pp. 821–824, Sep. 2016.

[7] Q. Zhao *et al.*, "Microring-based optical isolator and circulator with integrated electromagnet for silicon photonics," *J. Lightw. Techn.*, vol. 35, no. 8, pp. 1429–1437, Apr. 2017.

[8] E. Yablonovitch, "Inhibited spontaneous emission in solid-state physics and electronics," *Phys. Rev. Lett.*, vol. 58, no. 20, pp. 2059–2062, May 1987.

[9] S. John, "Strong localization of photons in certain disordered dielectric super-lattices," *Phys. Rev. Lett.*, vol. 58, no. 23, pp. 2486–2489, Jun. 1987.

[10] Z. Wang and S. H. Fan, "Optical circulators in two-dimensional magneto-optical photonic crystals," *Opt. Lett.*, vol. 15, no. 30, pp. 1989–1991, Aug. 2005.

[11] K. Yayoi, K. Tobinaga, Y. Kaneko, A. V. Baryshev, and M. Inoue, "Optical waveguide circulators based on two-dimensional magneto-photonic crystals: Numerical simulation for structure simplification and experimental verification," *J. Appl. Phys.*, vol. 109, no. 7, May 2011, Art. no. 07B750.

[12] V. Dmitriev, M. N. Kawakatsu, and F. J. de Souza, "Compact three-port optical two-dimensional photonic crystal-based circulator of W-format," *Opt. Lett.*, vol. 37, no. 15, pp. 3192–3194, Aug. 2012.

[13] X. Jin, Z. B. Ouyang, Q. Wang, M. Lin, and G. H. Wen, "Highly compact circulators in square-lattice photonic crystal waveguides," *PLos One*, vol. 9, no. 11, Nov. 2014, Art. no. e113508.

[14] V. Dmitriev, G. Portela, and L. Martins, "Photonic crystal-based circulators with three and four ports for sub-terzhertz region," *Photon. Netw. Commun.*, vol. 33, no. 3, pp. 303–312, Jun. 2017.

[15] F. Fan, S. J. Chang, C. Niu, Y. Hou, and X. H. Wang, "Magnetically tunable silicon ferrite photonic crystals for terahertz circulator," *Opt. Commun.*, vol. 285, no. 18, pp. 3763–3769, Aug. 2012.

[16] Y. Wang, D. G. Zhang, S. X. Xu, Z. B. Ouyang, and J. Z. Li, "Low-loss Y-junction two-dimensional magneto-photonic crystals circulator using a ferrite cylinder," *Opt. Commun.*, vol. 369, pp. 1–6, Jun. 2016.

[17] E. K. N. Yung, D. G. Zhang, and R. S. K. Wong, "A novel waveguide Y-junction circulator with a ferrite sphere for millimeter waves," *IEEE Trans. Microw. Theory Techn.*, vol. 44, no. 3, pp. 454–456, Mar. 1996.

[18] B. Owen, "The identification of modalresonances in ferrite loaded waveguide Y-junctions and their adjustment for circulation," *Bell Syst. Tech. J.*, vol. 51, no. 3, pp. 595–627, Mar. 1972.

[19] D. G. Zhang, "Design of partial height ferrites of H-plane waveguide circulator for given frequencies," *J. Chin. Inst. Commun.*, vol. 8, no. 6, pp. 56–59, Nov. 1987.

[20] Y. Wang, D. G. Zhang, S. X. Xu, B. G. Xu, Z. Dong, and T. Huang, "Experimental evidence of the large photonic band gap in two-dimensional square-lattice Al_2O_3 rods array," *Microw. Opt. Techn. Lett.*, vol. 59, no. 6, pp. 1347–1350, Jun. 2017.